REGULAR PAPER

Design, Simulation and Experiment for a Vortex-Induced Vibration Energy Harvester for Low-Velocity Water Flow

Dongxing Cao[1,2] · Xiangdong Ding[1,2] · Xiangying Guo[1,2] · Minghui Yao[3]

Abstract

Piezoelectric vibration energy harvesting has attracted considerable attention because of its prospects in self-powered electronic applications. There are a many low-velocity waters in nature, such as rivers, seas and oceans, which contain abundant hydrokinetic energy. In this paper, an optimal geometric piezoelectric beam combining magnetic excitation is identified and applied to a vortex-induced vibration energy harvester (ViVEH) for low velocity water flow, which is composed of a continuous variable-width piezoelectric beam carrying a cylindrical bluff body. The finite element simulation and experiment are first carried out to study the harvesting characteristics of the designed variable-width beam ViVEH without considering the magnetic excitation. The influence of the width-ratio and flow velocity on the harvesting voltage is studied in detail. The optimal structure, a ViVEH equipped with triangular piezoelectric beam, is then obtained by the superior energy harvesting performance for low velocity water flow. From the experimental results, at a flow velocity of 0.6 m/s, the highest root mean square (RMS) voltage and RMS voltage per unit area are 19.9 V and 0.07 V/mm^2, respectively. Furthermore, magnetic excitation is introduced to improve the scavenging performance of the optimal triangular beam ViVEH, different polarity arrangements are compared, and the optimal case, the arrangement of horizontal repulsion and vertical attraction (HR-VA), is obtained. This case can scavenge the highest power of 173 μW at a flow velocity of 0.5 m/s, which is increased by 127% compared to a conventional constant-width beam ViVEH with no magnetic excitation.

Keywords Energy harvesting · Low velocity flow · Vortex-induced vibration · Variable-width piezoelectric beam · Magnetic force enhancement

1 Introduction

In recent years, piezoelectric vibration energy harvesting (PVEH) has attracted considerable attention because of the prospects of piezoelectric vibration energy, a renewable and sustainable energy source, in self-powered electronic applications, such as remote wireless intelligent sensors and wearable and implantable medical devices [8, 10, 28, 29, 31, 39]. Many researchers have proposed various methods and structures to improve the harvesting efficiency, such as

bistable models [9, 11, 19, 25], tristable models [36, 37], multi-degree models [27, 32, 34], stochastic PVEH [13–15] and nonlinear internal resonance PVEH [5, 6, 12, 16].

Flowing fluid exists everywhere, and flow-induced vibration contains tremendous energy. Vortex-induced vibration (ViV) is one of the most common flow induced vibration phenomena, and can be used as a vibration energy source to power electronic devices located in remote or inconveniently accessible places. In terms of vortex-induced vibration energy harvesting, Akaydin et al. [1] investigated a self-excited piezoelectric energy harvester subjected to ViV oscillations. Dai et al. [7] and Zhang et al. [33] investigated the effects of circular cross-sections on the output efficiency and performance of a ViV harvester. Manfrida et al. [17] simulated nonlinear ViV energy converters, and the sensitivity to the stream velocity and the design parameters were investigated. Zhou and Wang [35] presented a novel dual serial vortex-induced vibration energy harvesting system for enhanced energy harvesting. Petrini and Gkoumas [21]

✉ Xiangying Guo
  eagle2008guo@yeah.net

1   College of Mechanical Engineering, Beijing University of Technology, Beijing 100124, China

2   Beijing Key Laboratory of Nonlinear Vibrations and Strength of Mechanical Structures, Beijing 100124, China

3   School of Artificial Intelligence, Tianjin Polytechnic University, Tianjin 300387, China

developed an analytical modeling and experimental wind tunnel test for a high-efficiency energy harvester. Zhou et al. [38] proposed a Y-shaped bistable energy harvester to scavenge low-speed wind energy. Wang et al. [30] studied a cross-coupled dual-beam structure for energy harvesting from ViV induced by wind flows in different directions.

The aforementioned studies mainly focused on energy harvesting from wind induced vibration. Bernitsas et al. [3] previously studied vortex-induced vibration aquatic clean energy which consists of a cylinder submerged perpendicular to water flows. Song et al. [24] studied upright piezoelectric cantilever beams for energy harvesting which was inspired by the ViV of a cylinder in flowing fluid. Qureshi et al. [22] designed a novel and scalable piezoelectric energy harvester for water pipelines. Recently, Sun et al. [26] studied piezoelectric energy harvesting from low-velocity water flow by vortex-induced vibration and galloping. Rezaei [23] presented a novel design of a PZT energy harvester for capturing energy from a broad range of vortex-shedding frequencies associated with varying wind speeds, which had a wider lock-in region and larger conversion factor than typical wake-galloping energy harvesters.

For vortex-induced VEHs, most research has focused on the effects of the bluff body, but for lower-velocity water flows, vortex-induced PVEHs have difficulty resonating because the vortex-induced force applied to the bluff body is small and the viscosity of water is high. In a divergence from existing literature, we combine the advantages of magnetic excitation from a lower-frequency VEH to a vortex-induced vibration energy harvester (ViVEH). Almost all conventional harvesting beams have been designed as constant-section beams. However, the piezoelectric effect induces of an electric charge in response to an applied mechanical strain and this effect relies heavily on the strain distribution of the harvester structure. Few researchers have studied the performance of VEHs with variable-section piezoelectric beams [2, 18, 20] and functionally graded piezoelectric beams [4]. The results have shown that a reasonable section shape of a piezoelectric beam could improve the strain

distribution, which could further increase the energy capture efficiently. Therefore, in this paper, we integrate a variable-section piezoelectric beam and magnetic excitation into a vortex-induced VEH, which can improve the power generation performance of a ViVEH for low-velocity water flow.

The paper is organized as follows. First, the physical model of the designed ViVEH with different variable-section beams is introduced. Both a finite element analysis and an experiment are then conducted to identify an optimal geometric beam for the proposed ViVEH. Furthermore, the energy harvesting performance of the optimal ViVEH with magnetic excitation under different water velocities is experimentally analyzed and the arrangement of the optimal polarity arrangement is obtained in Sect. 4, where the energy harvesting performance of the proposed ViVEH is discussed in detail. Finally, a discussion and conclusions are briefly given.

2 Structural Design and Experimental Setup

2.1 Structural Design

As mentioned above, the piezoelectric effect relies heavily on the strain distribution of the harvester structure. An optimal section shape of the piezoelectric beam can improve the strain distribution, which can further increase the energy capture efficiency. Therefore, a variable-width piezoelectric beam is regarded as the proposed energy harvesting structure, as shown in Fig. 1(a), which is a laminated beam consisting of a piezoelectric ceramic layer and substrate layer. Here, the materials of the piezoelectric and substrate layers are PZT-5H and phosphor bronze, respectively. The width of the fixed end and the free end are represented by b and a; thus, the variable-width beam model can be defined as the width-ratio a/b. In this paper, five cases of variable-width beam models are considered for discussion. In this paper, the value of dimension 'b' is fixed as 15 mm and different width ratios

Fig. 1 Schematic of **a** the variable-width piezoelectric beams and **b** the strain distribution
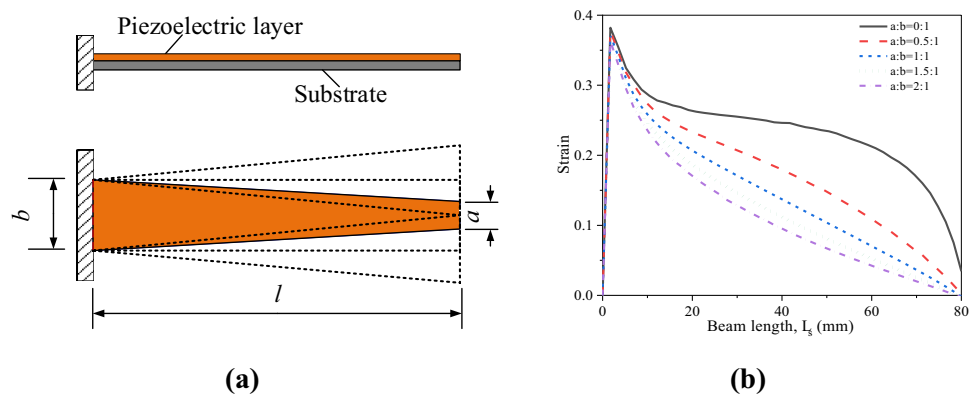
are achieved by changing dimension '*a*'. The values of the dimension '*a*' are chosen as 0 mm, 7.5 mm, 15 mm, 22.5 mm and 30 mm. The different width-ratios are then defined as a/b = 0, 0.5, 1.0, 1.5 and 2 with the dimension '*b*' determined as 15 mm. Based on a simple finite element analysis (FEA) by ANSYS workbench software, the strain distributions of variable-width piezoelectric beams with different width ratios are demonstrated in Fig. 1b. As the width ratio of *a:b* decreases, the strain distribution of the variable-section piezoelectric cantilever beams tends to be uniform. As a result, the triangular beam (the width-ratio is *a:b* = 0:1) can obtain the largest power generation per unit area among the five types of piezoelectric beams.

It is well known that low-velocity water flow widely exists in the natural environment. This paper focuses on the design of a highly efficient ViVEH for low-velocity water flow. A schematic diagram of the designed ViVEH is shown in Fig. 2a, which consists of a variable-width piezoelectric beam, a cylindrical bluff body and magnets. A 3D CAD model of the proposed ViVEH is shown in Fig. 2b. The ViVEH is placed in the flow field along water flow direction, and three pairs of magnets are attached to the bluff body and fixture. Each pair of magnets is placed in parallel. Here, magnetic excitation is introduced to improve the scavenging performance of the harvester. The purpose of the proposed design is to reduce the natural frequency and widen the bandwidth of the ViVEH, in other words, to reduce the critical vibration flow velocity and the broadband synchronization range of the flow velocity to resonate with the ViVEH.

Table 1 Material properties of the ViVEH

Parameters	Values
Mass of bluff body, m (g)	33
Length of substrate layer, L_s (mm)	80
Length of piezoelectric layer, L_P (mm)	35
Diameter of bluff body, D (mm)	25
Length of bluff body, L_C (mm)	30
Fluid density, ρ_f (kg/m^3)	1000
Magnet density, ρ_m (kg/m^3)	7400
Piezoelectric layer density, ρ_p (kg/m^3)	7600
Substrate layer density, ρ_s (kg/m^3)	8300
Young modulus of the piezoelectric layer, E_p (GPa)	15.857
Young modulus of the elastic beam, E_s (GPa)	110
Piezoelectric constant, d_{31} (pC/N)	−210
Magnet type	N50
Residual induration, B_r (KGs)	14.5

In this paper, the thicknesses of the substrate layer and the piezoelectric layer are all 0.2 mm. The other material parameters are listed in Table 1.

It is important to obtain the frequency characteristics of the variable-width piezoelectric beam with a bluff body for the ViVEH without magnetic excitation. Therefore, the FEA of harmonic responses from the ANSYS workbench is studied first, and the bluff body is treated as an additional tip mass with heavier weight. The amplitude-frequency response of the structure with a bluff body is just the opposite of the structure without a bluff body, as shown in Fig. 3. It is shown that the natural frequency of the ViVEH gradually decreases as the width ratio decreases. For a triangular
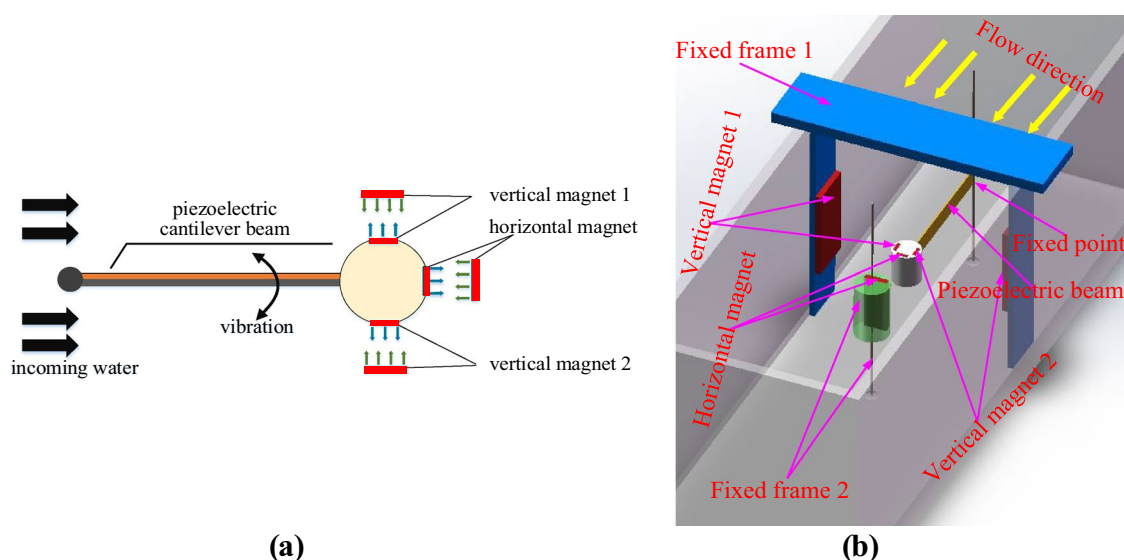

Fig. 2 Physical model of the proposed ViEVH: **a** schematic diagram; **b** 3D CAD model
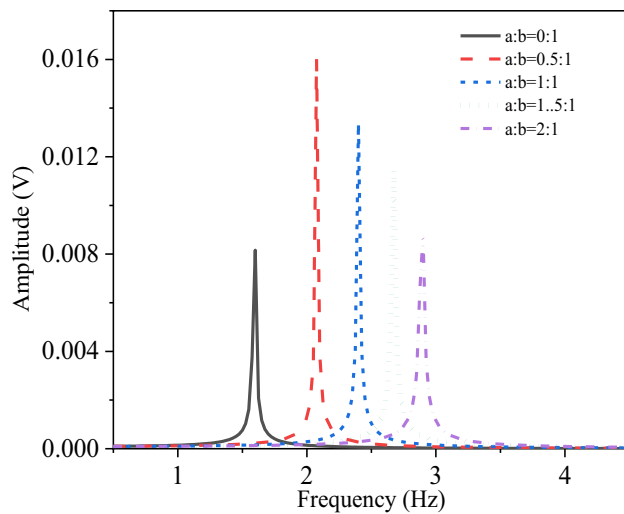
Fig. 3 Amplitude-frequency response (FEA result) of variable-width piezoelectric beams with a bluff body

beam, the natural frequency is 1.6 Hz, which is the lowest natural frequency among the five cases of the variable-width piezoelectric beam.

2.2 Experimental Setup

Figure 4 shows the schematic diagram and prototype of the experimental system, which is essentially a water circulation system, including a water supply system and an experimental flume system. As shown in Fig. 4a, the water supply system includes a water storage device, a water pump and pipes, an experimental flume system includes a flow stabilization device, a diffusion device, an experimental flume, and an outlet gate. The water pump is used to transport water to the flume, where the valves are used to control the water volume of the experimental flume. The motor is also applied to control the hanging door of the outlet gate. Thus the water velocity in the flume can be precisely adjusted. The flow velocity is measured synchronously using a current meter. A piezoelectric beam, such as a ViVEH, is clamped in the fixed frame and completely immersed in water. During the experiment, a digital oscilloscope is used to observe the scavenging voltage.

Figure 4b, c shows the experimental platform and the ViVEH prototype, respectively. Three exciting magnets are mounted on the fixture; two are placed on the left and right sides of the bluff body, and one is placed behind the bluff body. The three excited magnets are embedded into the bluff body and aligned parallel to the exciting magnet on the fixture. Thus, there will be an attractive force between unlike poles and the repulsive force between like poles to provide the bluff body with magnetic forces from the left, right, and back. At the same time, to ensure the insulation

characteristics of the ViVEH, the piezoelectric cantilever beam needs to be waterproof.

3 Finite Element (FE) Simulation and Experiment for the Designed ViVEH

3.1 FE Simulation for the Designed ViVEH

In this section, without considering the magnetic excitation, the FE simulation for the designed ViVEH with various width-ratios is conducted to demonstrate the energy harvesting performance by using the mechanical and fluent modules in the ANSYS workbench. As shown in Fig. 5a, the ViVEH is placed in the cuboid water flow field along the flow direction of the fluid. The flow field model includes an inlet, boundary, and outlet. The length, width, and height of the cuboid flow field are 400 mm, 150 mm, and 50 mm, respectively. The influence of the width ratio and flow velocity on the scavenging voltage of the ViVEH are investigated in detail. First, Fig. 5b–f shows the output voltage waveforms for the five width ratio cases when the flow velocity $U = 0.5$ m/s. Here, the output voltage obtained by the FE simulation is for the open-circuit condition. In the following content, if not specified, all output voltages indicate open-circuit voltage. The results indicate that the ViVEH starts to vibrate slowly under the action of vortex excitation with the increasing calculation time of fluid–structure coupling, and the output voltage gradually increases and stabilizes.

Combining Fig. 5b–f together, as shown in Fig. 6, demonstrates the influence of the width ratio on the output voltage. When the water flow velocity is 0.5 m/s, the output voltage waveforms indicate that the output voltage gradually increases as the width-ratio decreases. The frequency of the ViVEH gradually decreases as the width-ratio decreases based on the FFT results. The minimum vibration frequency and the maximum voltage amplitude of the ViVEH are 2.25 Hz and 8.6 V, respectively, when the width-ratio becomes zero. Fluid–structure coupling FEA results show that the ViVEH with a triangular piezoelectric beam has the largest output voltage and lowest vibration frequency. Correspondingly, it is better to match the lower critical flow velocity, which can vibrate to obtain superior energy harvesting performance.

Figure 7 shows the influence of flow velocity on the amplitude of output voltage and the amplitude of output voltage per unit area with different width ratios. The results, as shown in Fig. 7a, indicate that the amplitude of the output voltage gradually increases with increasing flow velocity in general. However, for width ratios of 1.5 and 2.0, the amplitude of the output voltage decreases when the flow velocity is faster than 0.6 m/s. It is easy to understand that the voltage cannot increase without restraint due to the limitation of
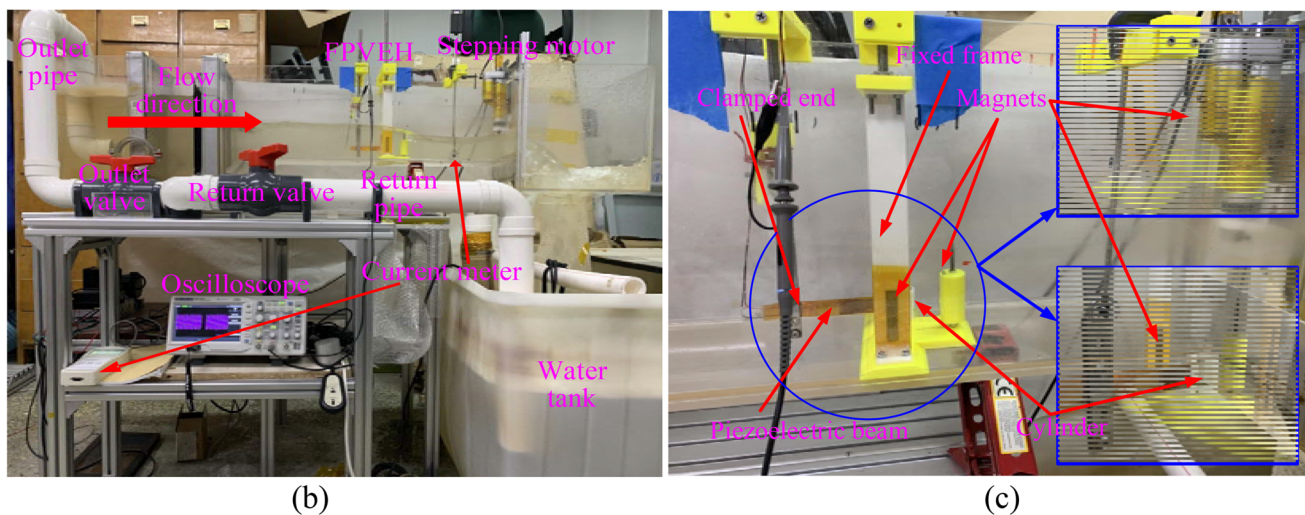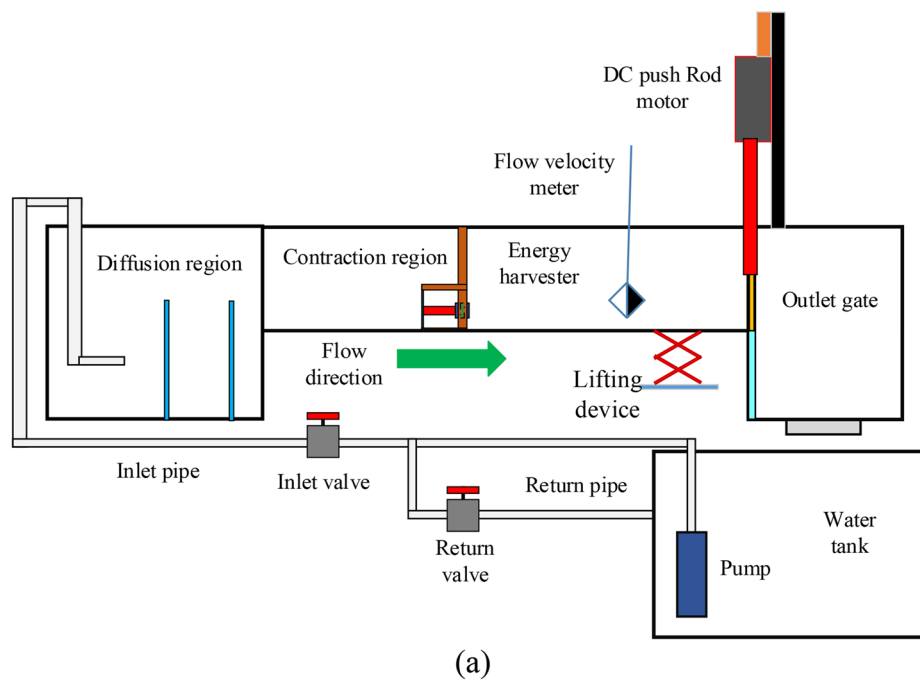
Fig. 4 Experimental platform: **a** schematic diagram; **b** experimental platform; **c** prototype of the proposed ViVEH

resonance frequency and the existence of a lock-in region. There are different vortex-induced shedding frequencies at different flow velocities, therefore, there is a maximum voltage for each ViVEH with a certain width-ratio. In other words, the output voltage of ViVEHs with different width ratios can reach a maximum value only at a certain flow velocity. Overall, the ViVEH with a triangular beam has the highest amplitude of output voltage, which reaches 9.4 V when the flow velocity is 0.6 m/s.

In this paper, piezoelectric material covers the entire beam surface, so the piezoelectric layer is different for different width-ratio beams. It is more reasonable and meaningful

to discuss the power generation capacity on the unit area of the piezoelectric material. As shown in Fig. 7b, it is obvious that the energy harvesting performance of the triangular beam ViVEH is preferable to the other width ratio beams in the range of full experimental flow velocity. The highest voltage amplitude per unit area, 0.035 V/mm^2; occurs when the flow velocity is 0.6 m/s.

3.2 Experimental Studies for the Designed ViVEH

In this section, the experiment is conducted to study the influences of structure and flow parameters on the designed
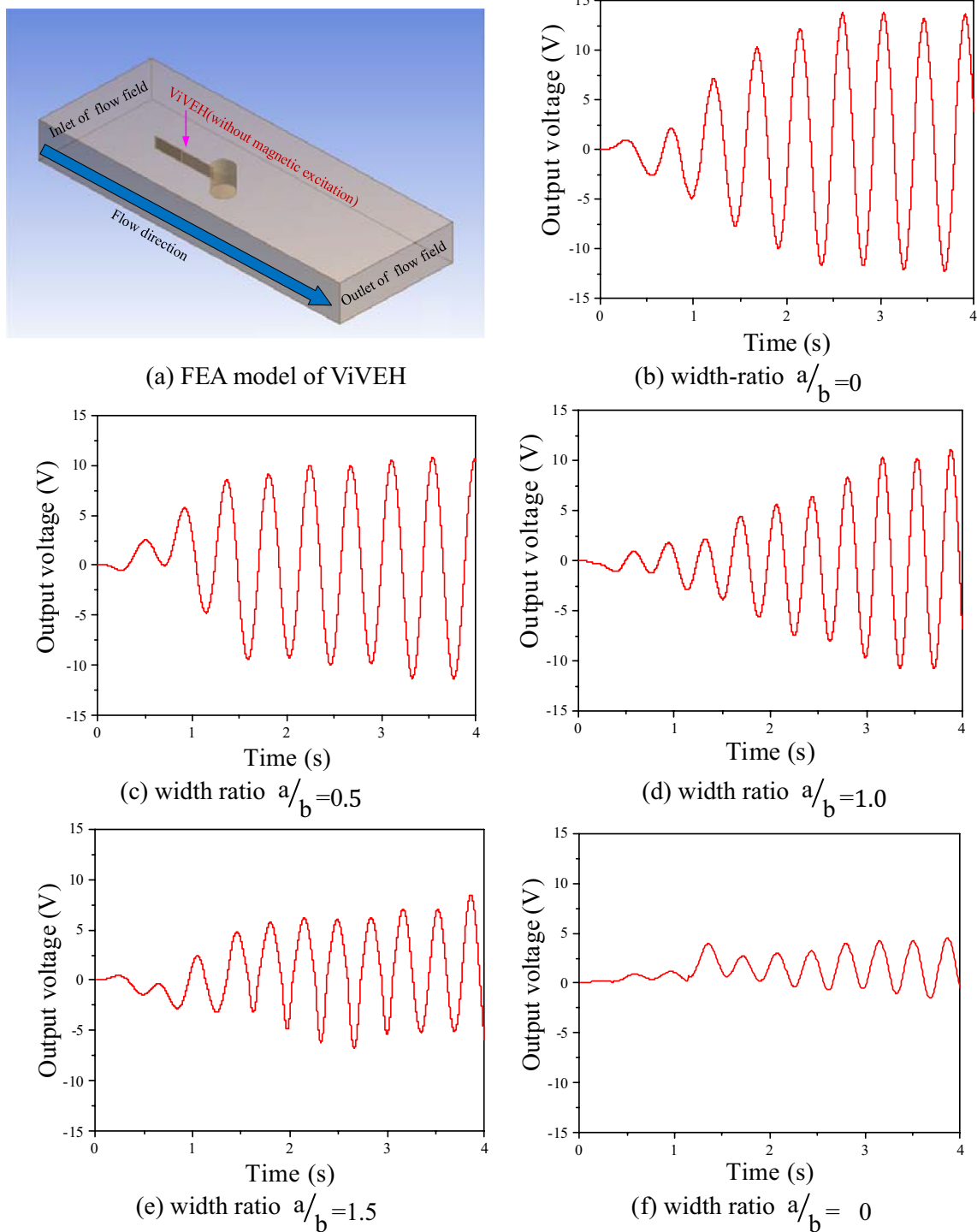
(a) FEA model of ViVEH

(b) width-ratio $a/b = 0$

(c) width ratio $a/b = 0.5$

(d) width ratio $a/b = 1.0$

(e) width ratio $a/b = 1.5$

(f) width ratio $a/b = 0$

Fig. 5 FEA model of the ViVEH and numerical results for the output voltage waveform at $U = 0.5$ m/s

ViVEH without magnetic excitation. Figure 8 shows the time history of the output voltage at different flow velocities of 0.1 m/s, 0.3 m/s, 0.55 m/s and 0.7 m/s. This indicates that the highest voltage occurs when the flow velocity is 0.55 m/s. Taking a flow velocity of 0.5 m/s as an example,

Fig. 9 demonstrates the influence of the width ratio on the output voltage. The results show that the output voltage gradually increases as the width ratio gradually decrease, while the vibration frequency of the ViVEH gradually decreases at the same time. Compared with Fig. 6, it can
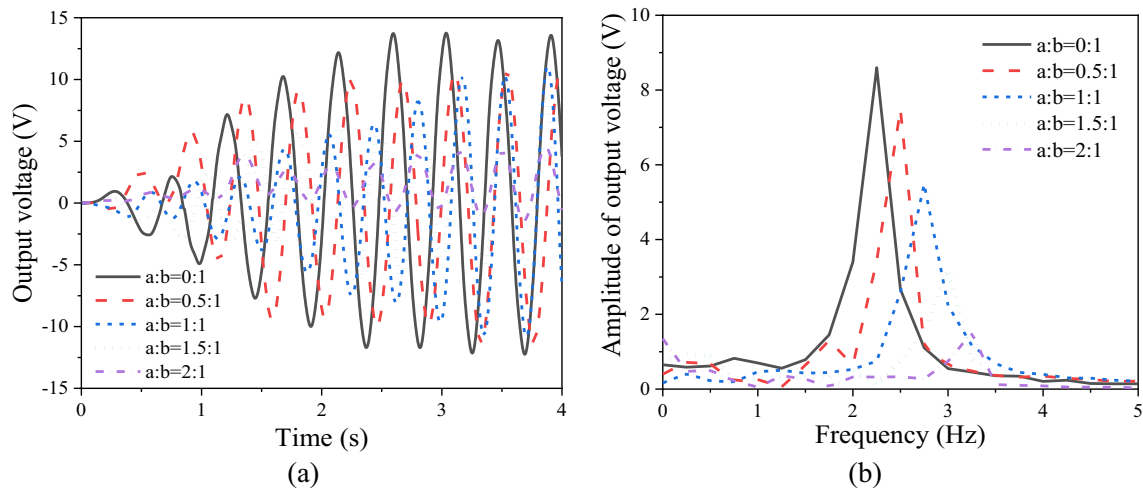
Fig. 6 Influence of width-ratio on output voltage: **a** the voltage waveforms, **b** the FFT results
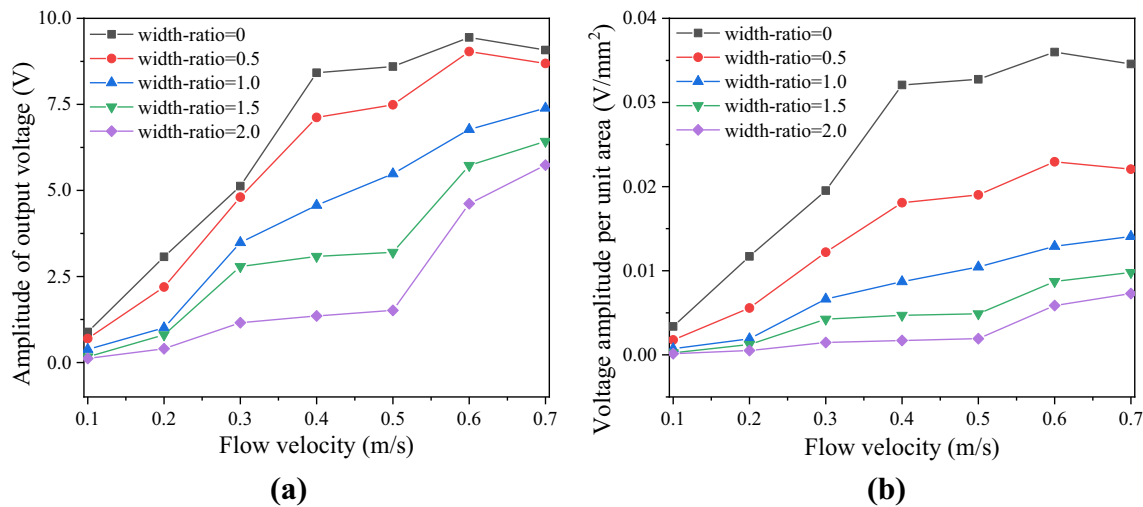

Fig. 7 Numerical results for the influence of flow velocity on: **a** amplitude of output voltage, **b** voltage amplitude per unit area
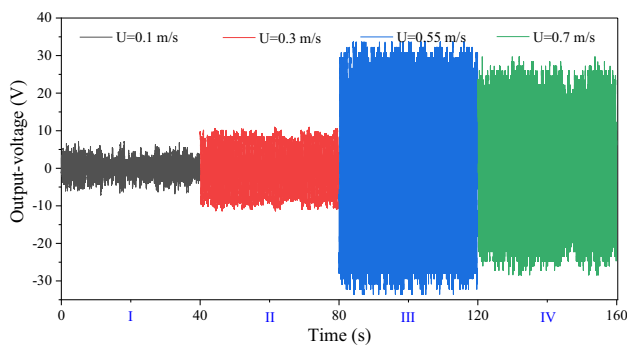

Fig. 8 Time history of the experimental output voltage at different flow velocities

be seen that there is good agreement between the FEA and the experimental results. Here, the minimum output voltage frequency and the maximum output voltage of the ViVEH are 2.025 Hz and 13.0 V, respectively. It is obvious that the ViVEH with triangular piezoelectric beam has the highest output voltage and lowest vibration frequency. The reason is that the structure of the ViVEH with a triangular piezoelectric beam has the most uniform strain distribution and the lowest natural frequency.

Figure 10 shows the influence of flow velocity on the output RMS voltage and the frequency with different width ratios. It is obvious that the output voltage of the ViVEH mainly increases as the flow velocity increases. However,
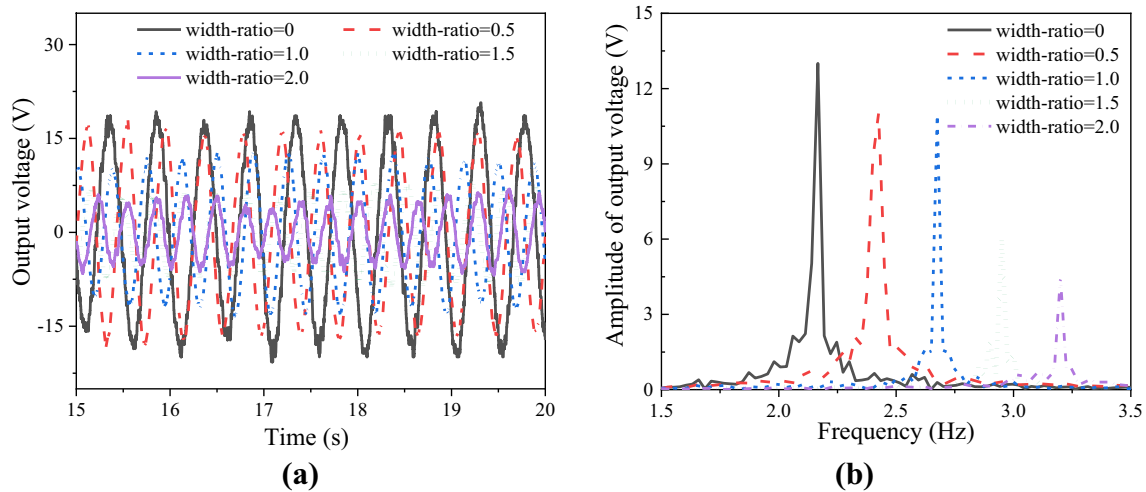
Fig. 9 The influence of width ratio on the ViVEH, **a** the voltage waveforms; **b** the FFT results

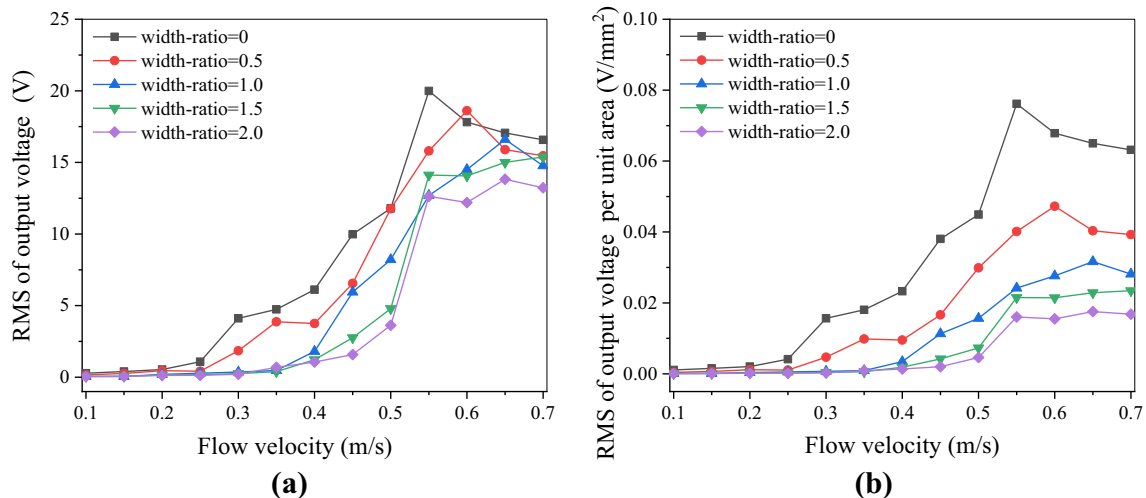**Fig. 10** Experimental results for the influence of flow velocity on: **a** the output RMS voltage and b the output RMS voltage per unit area

when the vortex-induced shedding frequency reaches the natural frequency of the ViVEH, the output voltage reaches the maximum value and enters the lock-in region. Here, the triangular beam ViVEH obtain the highest output voltage −19.9 V when the flow velocity is 0.6 m/s. It can also be seen that the triangular cantilever beam has the lowest vibration frequency at different flow velocities. Moreover, considering the voltage on the unit piezoelectric area, the triangular beam ViVEH also achieves the highest RMS output voltage, reaching 0.07 V/mm². Compared with Fig. 7, the experimental results are consistent with the FEA results in Sect. 3.1. This indicates that the triangular beam ViVEH exhibits excellent performance.

Based on the above analysis, it is obvious that the triangular piezoelectric beam is the optimal structure for the

ViVEH. To validate the correctness of the experimental and numerical results, we choose the triangular piezoelectric beam as an example. A comparison of the experimental and numerical results at 0.5 m/s flow velocity is shown in Fig. 11. As indicated, there is good agreement between the experimental and numerical results.

4 Performance of the Optimal ViVEH with Magnetic Excitation

In this section, magnetic excitation is introduced to improve the performance of the optimal ViVEH, as numerous studies have investigated the VEH from base excitation. Here, the magnets are arranged as in the layout for Fig. 2, which
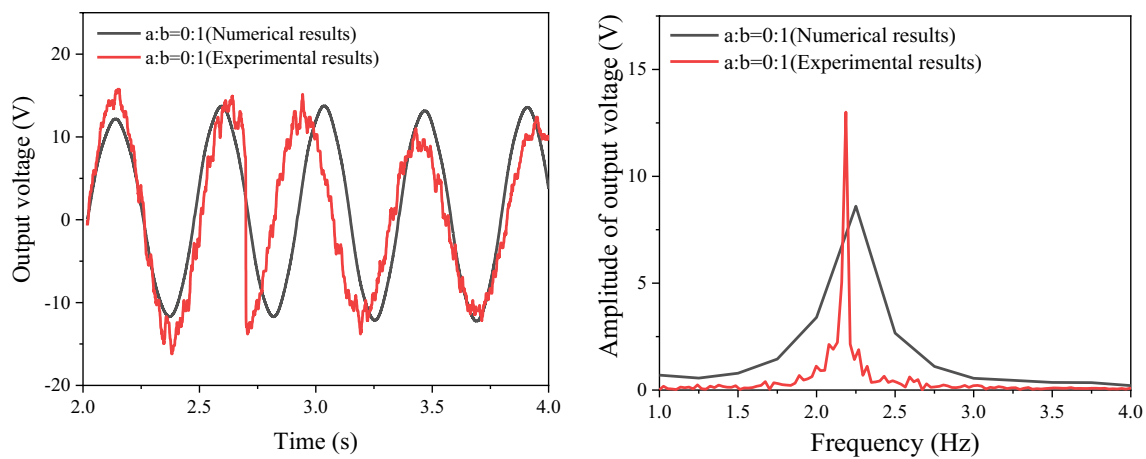
Fig. 11 Comparison between the experimental and numerical results: **a** the voltage waveforms; **b** the FFT results

has 2 vertical magnets and 1 horizontal magnet. The magnets, which are movable with the vibration of the beam and bonded into the bluff body, are excited magnets. The other magnets that are fixed in the frame are exciting magnets. According to the properties of excited and exciting magnets, where like poles repel and unlike poles attract, the magnetic force exerted on the bluff body can be classified as horizontal repulsion and vertical attraction (HR-VA), horizontal attraction and vertical attraction (HA-VA), horizontal repulsion and vertical repulsion (HR-VR), and horizontal attraction and vertical repulsion (HA-VR). The effect of the magnetic distance on the energy harvesting performance can be obtained based on numerous VEH studies from base excitation. In this paper, the magnetic distance between the excited magnet and exciting magnet is determined, to avoid the adsorption phenomenon caused by an excessively large magnetic force from vertical magnets, and the magnetic distance of the vertical magnets is determined to be 40 mm. In addition, to avoid the vortex-induced shedding being disturbed due to the distance of the fixed frame being too close to the bluff body, the magnetic distance of the horizontal magnets is determined to be 30 mm. The effective width, length and thickness of the excited magnets are 9 mm, 30 mm and 2.8 mm, respectively. In addition, the effective width, length and thickness of the exciting magnets are 15 mm, 30 mm and 2.8 mm, respectively.

Figure 12 demonstrates the time history of the output voltage for the HR-VA case under different flow velocities. This indicates that the highest voltage occurs when the flow velocity is 0.5 m/s. Taking the flow velocity of 0.5 m/s as an example, Fig. 13a shows the output voltage for all cases of magnetic excitation. For this determined flow velocity, Fig. 13b shows the FFT voltage results. The orders of the output voltage and the vibration frequencies of the ViVEHs with magnetic forces are HR-VA > HA-VA > HR-VR > HA-VR and HR-VA < HA-VA < HR-VR < HA-VR, respectively.
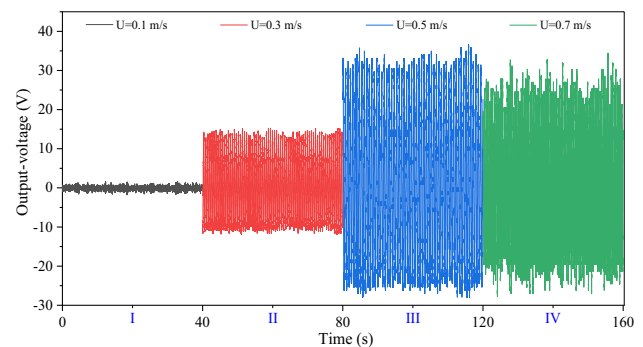

Fig. 12 Experimental time history of the output voltage at different flow velocities

The ViVEH with HR-VA magnets has the largest voltage amplitude (20.5 V) and lowest frequency (1.452 Hz). It is also apparent that the output voltage and lowest frequency of the HR-VA layout are higher and lower than those of the ViVEH with no magnetic excitation, respectively. For brevity, Fig. 13c provides a comprehensive demonstration of the RMS output voltage and frequency for all cases of magnetic excitation. Similar to the results in Sect. 3, the output voltage gradually increases with increasing flow velocity. The voltage reaches a maximum value when the vortex-induced shedding frequency reaches the natural frequency of the ViVEH. The vibration of the ViVEH will remain in the lock-in region, and the voltage decreases as the flow velocity increases. Here, it is obvious that the ViVEH with the HR-VA magnets has the highest RMS output voltage, which is 20.9 V when the flow velocity is 0.55 m/s. It can also be seen that the HR-VA layout has the lowest vibration frequency at different flow velocities.

The aforementioned experimental results demonstrate that the triangular piezoelectric beam ViVEH with HR-VA magnets exhibits the best energy harvesting performance
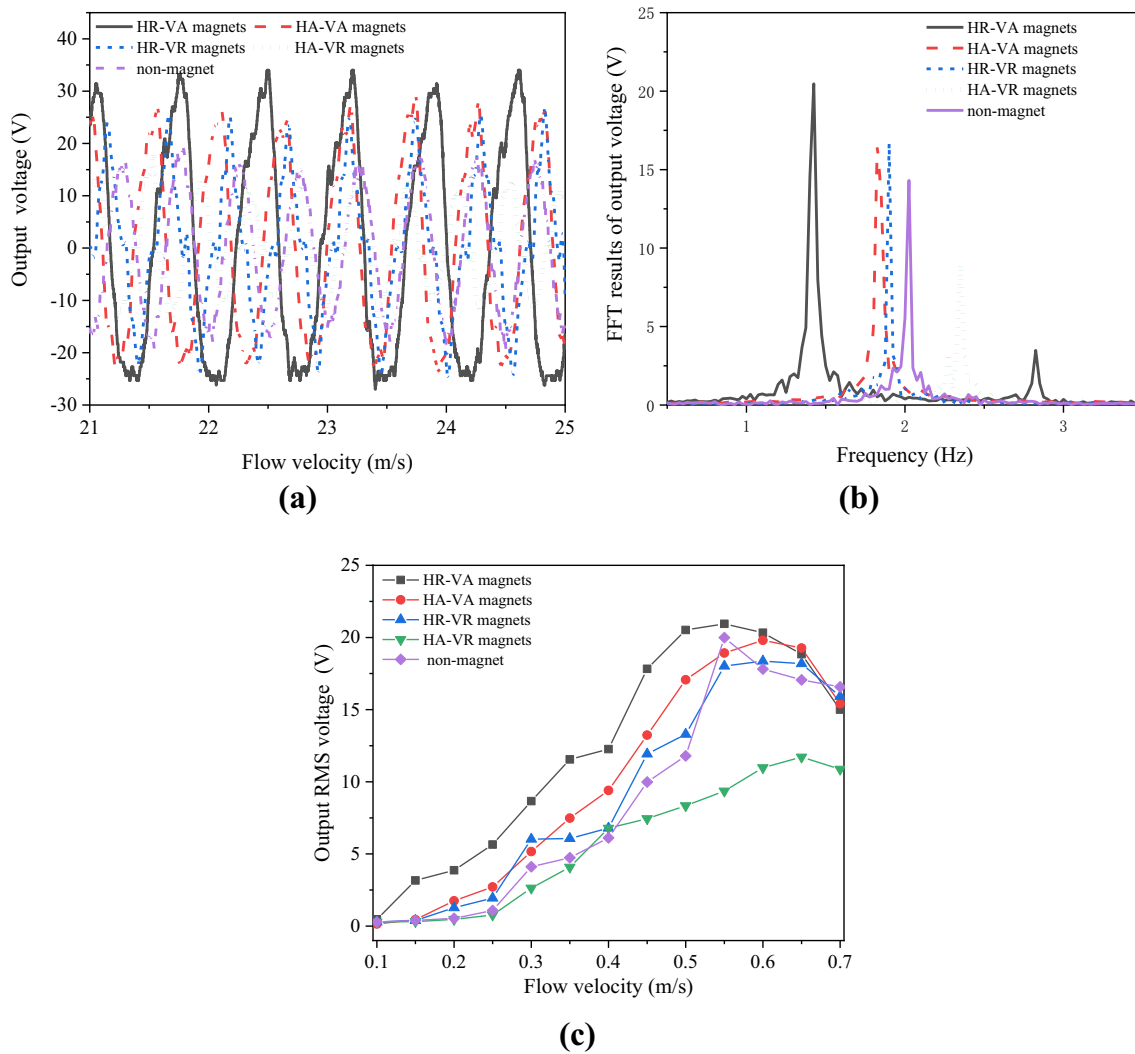
Fig. 13 Experimental result for the influence of polarity magnets on the ViVEH: **a** voltage waveforms; **b** FFT results; **c** output RMS voltage

for low-velocity water flow. Thus far, the proposed optimal ViVEH is defined as the integration of the triangular piezoelectric beam and the HR-VA magnets. Now, we focus on a comparison of four typical ViVEHs: the triangular/rectangular piezoelectric beam ViVEH with HR-VA magnets and conventional constant-width piezoelectric beam ViVEH with/without magnetic excitation. Figure 14 shows the comparison results of the four ViVEH cases. The output voltage for all cases of magnetic excitation at 0.5 m/s flow velocity is demonstrated in Fig. 14a. For this determined flow velocity, the FFT voltage result is demonstrated in Fig. 14b. As shown in Fig. 14a, b, the rectangular piezoelectric beam ViVEH with HR-VA magnets has the highest output voltage, which is 25.8 V. It is increased by 50% compared to the rectangular piezoelectric beam ViVEH without magnets. The triangular piezoelectric beam ViVEH with HR-VA magnets has the lowest frequency, which is 1.425 Hz. It is decreased

by 48.6% compared to the rectangular piezoelectric beam ViVEH without magnets. The experimental results indicate that the optimal shape of the piezoelectric beam can reduce the natural frequency and that the HR-VA layout can increase the output voltage of the ViVEH. The RMS output voltage for all cases of magnetic excitation is shown in Fig. 14c. It is obvious that the triangular piezoelectric beam ViVEH with HR-VA magnets has a higher RMS output voltage than the other three cases, especially at low flow velocities. Considering the RMS voltage on the unit piezoelectric area, as shown in Fig. 14d, the RMS voltage per unit area reaches its highest value of 0.079 V/mm^2 at 0.5 m/s flow velocity, which is a 163% increase. It is obvious that the triangular beam ViVEH has the best energy harvesting performance compared to a conventional constant-section ViVEH with no magnet.

External resistance is an important parameter affecting the output characteristics of the energy harvester;
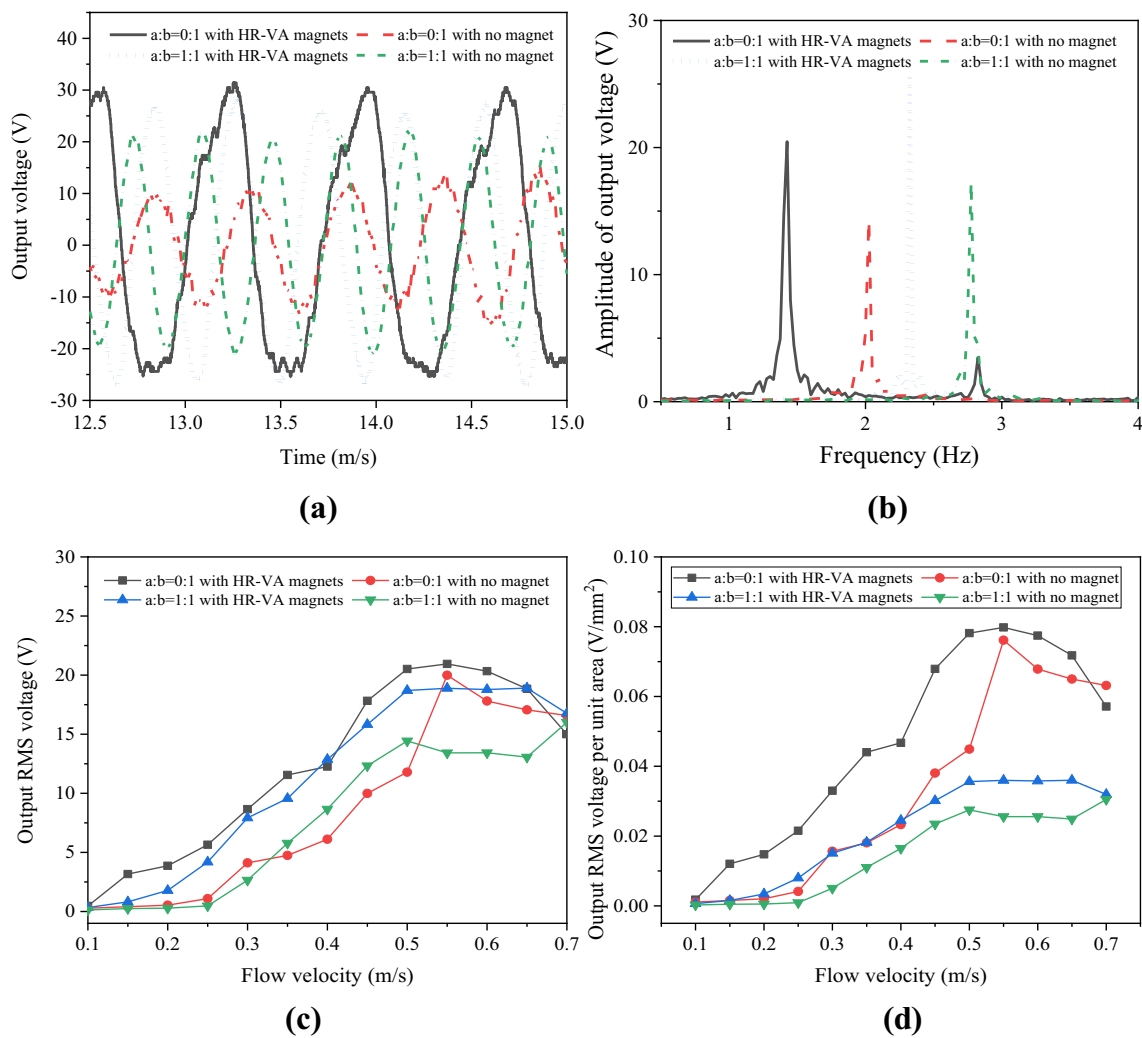
Fig. 14 Experimental comparison of the output voltage between the optimal and conventional ViVEHs, **a** the voltage waveforms; **b** the FFT results; **c** the output RMS voltage; **d** the output RMS voltage per unit area

thus, external resistance is employed to discuss the output performance, as shown in Fig. 15. The output voltage under load resistors and output power are demonstrated in Fig. 15a, b, respectively. As the resistance value increases, the output RMS voltage increases and then stabilizes. However, as the resistance value increases, the output power increases first and then decreases, so there is an optimal impedance value that achieves the maximum output power, which is approximately 600 KΩ. Moreover, the triangular beam ViVEH with HR-VA has the highest output power of 173 μW at a flow velocity of 0.5 m/s. It is increased by 127% compared to a conventional constant-width beam ViVEH with no magnet. Figure 15c, d shows the output voltage and power per unit area, respectively. Here, the highest power per unit area of the three ViVEH cases are 0.66 μW, 0.23 μW and 0.14 μW, respectively. It

is obvious that the triangular beam ViVEH with HR-VA has significant superiority over the other two cases.

In this section, the optimal layout of the magnets, HR-VA magnets, is first identified based on the experimental results. The proposed optimal ViVEH is then determined and the experiment is conducted to test the advantages. Compared with the conventional constant-width piezoelectric beam ViVEH without magnets, the proposed optimal ViVEH demonstrates superiority in both output voltage and frequency for lower flow velocity. The output voltage and power per unit area are much more remarkable, as shown in Fig. 15c, d.
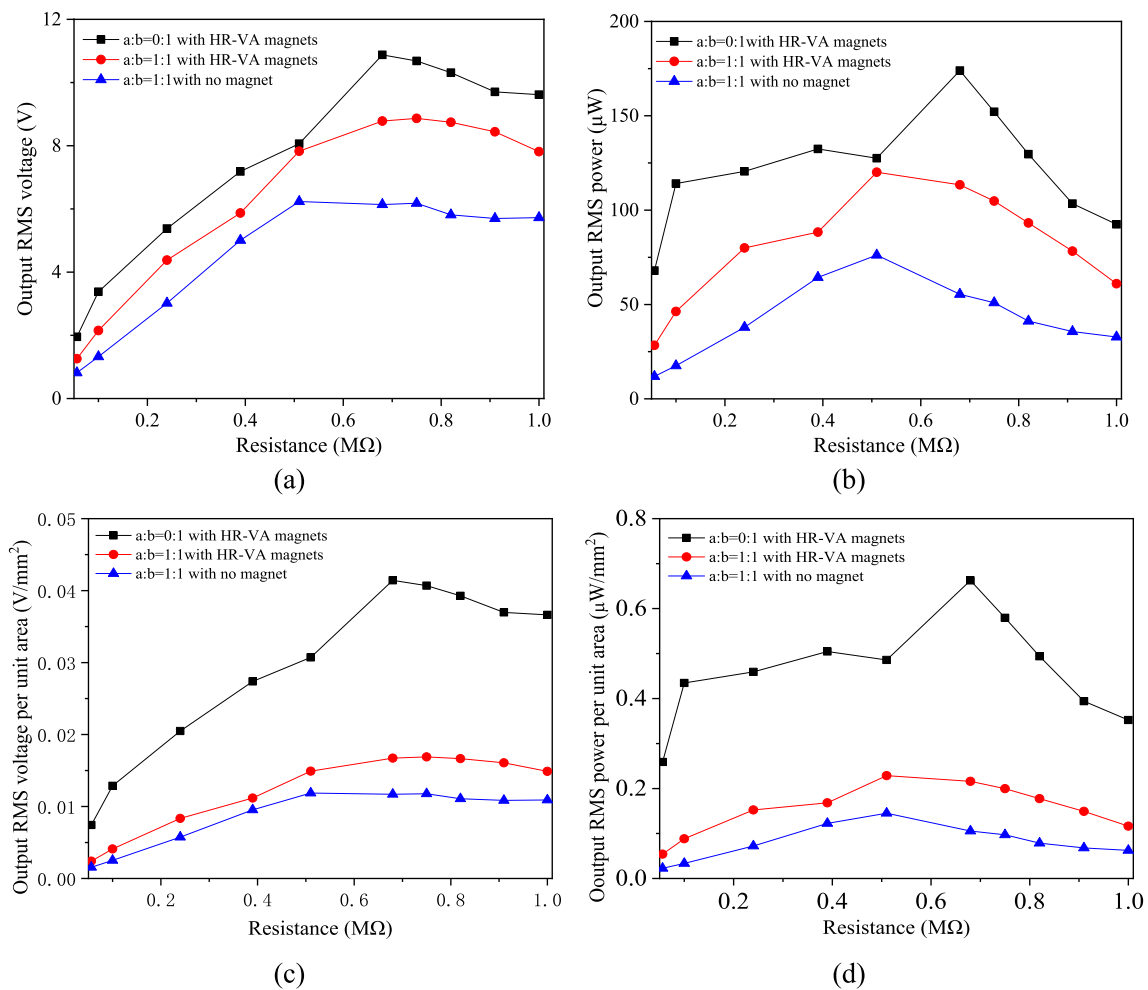
Fig. 15 Experimental comparison of the output power between the optimal and conventional ViVEH: **a**, **b** for output RMS voltage and power, respectively; **c**, **d** for output RMS voltage and power per unit area, respectively

5 Conclusions

In this work, a ViVEH for low-velocity water flow is proposed. The system is composed of a variable-width piezoelectric beam carrying a cylindrical bluff body. Meanwhile, magnetic force excitation is also introduced to improve the harvesting performance. The strain distribution of variable-width piezoelectric beams is first analyzed by FEA to indicate that the triangular-width piezoelectric beam has superior mechanical properties for vibration energy harvesters compared to conventional constant-width piezoelectric beams. Then a finite element simulation and experiment for a ViVEH with variable-width piezoelectric beams are presented and agree well. The triangular beam ViVEH demonstrates its advantages, especially in low velocity water flow, and scavenges its maximum voltage at an optimal flow velocity of 0.55 m/s. The highest harvested RMS voltage and per unit area RMS voltage are 20.9 V and 0.079 V/mm^2, respectively. Furthermore, the effect of magnetic force on

the optimal ViVEH with the triangular piezoelectric beam is experimentally studied. The results show that the magnetic excitation can reduce the system frequency and that the HR-VA magnet case has the best energy harvesting performance for low velocity water flow. In this case, the output voltage and the critical velocity needed to vibrate the ViVEH with a triangular piezoelectric cantilever beam are the highest and lowest, respectively. Moreover, the effect of resistance on the harvesting performance of the optimal ViVEH is also discussed. It scavenges the highest power of 173 µW at a flow velocity of 0.5 m/s, which is increased by 127% compared to the conventional constant-width beam ViVEH with no magnet. At the same time, the results indicates that the triangular piezoelectric beam ViVEH with HR-VA magnets has much lower critical flow velocity, which is decreased by 48.6%, and much higher output power per unit area, which is increased by 371.4% compared to the conventional constant-section ViVEH with no magnet. The results demonstrated that the maximum power of the proposed ViVEH, in all of

the considered cases, is improved considerably. Based on the excellent energy harvesting performance, the proposed integrated ViVEH can be used for the further optimization of a vortex-induced vibration energy harvester for lower velocity water flow.

Compliance with Ethical Standards

Conflict of interest On behalf of all authors, the corresponding author states that there is no conflict of interest.

References

1. Akaydin, H. D., Elvin, N., & Andreopoulos, Y. (2012). The performance of a self-excited fluidic energy harvester. *Smart Materials and Structures, 21*, 025007.
2. Ben Ayed, S., Abdelkefi, A., Najar, F., et al. (2014). Design and performance of variable-shaped piezoelectric energy harvesters. *Journal of Intelligent Material Systems and Structures, 25*, 174–186.
3. Bernitsas, M. M, Raghavan, K., Ben-Simon, Y., et al. (2008). VIVACE (Vortex Induced Vibration Aquatic Clean Energy): A new concept in generation of clean and renewable energy from fluid flow. *Journal of Offshore Mechanics and Arctic Engineering, 130*.
4. Bodaghi, M., Damanpack, A. R., Aghdam, M. M., et al. (2014). Geometrically non-linear transient thermo-elastic response of FG beams integrated with a pair of FG piezoelectric sensors. *Composite Structures, 107*, 48–59.
5. Cao, D. X., Leadenham, S., & Erturk, A. (2015). Internal resonance for nonlinear vibration energy harvesting. *European Physical Journal-Special Topics, 224*, 2867–2880.
6. Chen, L. Q., & Jiang, W. N. (2015). A piezoelectric energy harvester based on internal resonance. *Acta Mechanica Sinica, 31*, 223–228.
7. Dai, H., Abdelkefi, A., & Wang, L. (2014). Theoretical modeling and nonlinear analysis of piezoelectric energy harvesting from vortex-induced vibrations. *International Journal of Mechanical Sciences, 25*, 1861–1874.
8. Daqaq, M. F., Masana, R., Erturk, A., et al. (2014). On the role of nonlinearities in vibratory energy harvesting: A critical review and discussion. *Applied Mechanics Reviews, 66*, 045501.
9. Erturk, A., Hoffmann, J., & Inman, D. J. J. A. P. L. (2009). A piezomagnetoelastic structure for broadband vibration energy harvesting. *Applied Physics Letters, 94*, 254100–254102.
10. Jin, J. W., Kang, K. W., & Kim, J. H. (2015). Development of durability test procedure of vibration-based energy harvester in railway vehicle. *International Journal of Precision Engineering and Manufacturing-Green Technology, 2*, 353–358.
11. Kim, J. E., Lee, S., & Kim, Y. Y. (2019). Mathematical model development, experimental validation and design parameter study of a folded two-degree-of-freedom piezoelectric vibration energy harvester. *International Journal of Precision Engineering and Manufacturing-Green Technology, 6*, 893–906.
12. Lan, C. B., Qin, W. Y., & Deng, W. Z. (2015). Energy harvesting by dynamic unstability and internal resonance for piezoelectric beam. *Applied Physics Letters, 107*, 093902.
13. Liu, D., Xu, Y., & Li, J. L. (2017). Probabilistic response analysis of nonlinear vibration energy harvesting system driven by Gaussian colored noise. *Chaos Solitons & Fractals, 104*, 806–812.
14. Liu, D., Xu, Y., & Li, J. L. (2017). Randomly-disordered-periodic-induced chaos in a piezoelectric vibration energy harvester system with fractional-order physical properties. *Journal of Sound and Vibration, 399*, 182–196.
15. Lu, Z. Q., Chen, L. Q., Brennan, M. J., et al. (2016). Stochastic resonance in a nonlinear mechanical vibration isolation system. *Journal of Sound and Vibration, 370*, 221–229.
16. Lu, Z. Q., Ding, H., & Chen, L. Q. (2019). Resonance response interaction without internal resonance in vibratory energy harvesting. *Mechanical Systems and Signal Processing, 121*, 767–776.
17. Manfrida, G., Rinchi, M., & Soldi, G. (2016). Dynamic model of a vortex-induced energy converter. *Energy Resources Technology, 138*, 062002.
18. Muthalif, A. G. A., & Nordin, N. H. D. (2015). Optimal piezoelectric beam shape for single and broadband vibration energy harvesting: Modeling, simulation and experimental results. *Mechanical Systems and Signal Processing, 54–55*, 417–426.
19. Nguyen, M. S., Yoon, Y.-J., & Kim, P. (2019). Enhanced broadband performance of magnetically coupled 2-DOF bistable energy harvester with secondary intrawell resonances. *International Journal of Precision Engineering and Manufacturing-Green Technology, 6*, 521–530.
20. Ooi, B. L., Gilbert, J. M., & Aziz, A. R. (2016). Analytical and finite-element study of optimal strain distribution in various beam shapes for energy harvesting applications. *Acta Mechanica Sinica, 32*, 670–683.
21. Petrini, F., & Gkoumas, K. (2018). Piezoelectric energy harvesting from vortex shedding and galloping induced vibrations inside HVAC ducts. *Energy and Buildings, 158*, 371–383.
22. Qureshi, F. U., Muhtaroğlu, A., & Tuncay, K. (2017). Near-optimal design of scalable energy harvester for underwater pipeline monitoring applications with consideration of impact to pipeline performance. *IEEE Sensors Journal, 17*, 1981–1991.
23. Rezaei, M., & Talebitooti, R. (2019). Wideband PZT energy harvesting from the wake of a bluff body in varying flow speeds. *International Journal of Mechanical Sciences, 163*, 105135.
24. Song, R., Shan, X., Lv, F., et al. (2015). A study of vortex-induced energy harvesting from water using PZT piezoelectric cantilever with cylindrical extension. *Ceramics International, 41*, S768–S773.
25. Sun, S., & Cao, S. Q. (2017). Analysis of chaos behaviors of a bistable piezoelectric cantilever power generation system by the second-order Melnikov function. *Acta Mechanica Sinica, 33*, 200–207.
26. Sun, W., Zhao, D., Tan, T., et al. (2019). Low velocity water flow energy harvesting using vortex induced vibration and galloping. *Applied Energy, 251*, 113392.
27. Sun, X., Wang, F., & Xu, J. (2019). Nonlinear piezoelectric structure for ultralow-frequency band vibration energy harvesting with magnetic interaction. *International Journal of Precision Engineering and Manufacturing-Green Technology, 6*, 671–679.
28. Tri Nguyen, H., Genov, D. A., & Bardaweel, H. (2020). Vibration energy harvesting using magnetic spring based nonlinear oscillators: Design strategies and insights. *Applied Energy, 269*, 115102.
29. Usharani, R., Uma, G., & Umapathy, M. (2016). Design of high output broadband piezoelectric energy harvester with double tapered cavity beam. *International Journal of Precision Engineering and Manufacturing-Green Technology, 3*, 343–351.
30. Wang, J., Hu, G., Su, Z., et al. (2019). A cross-coupled dual-beam for multi-directional energy harvesting from vortex induced vibrations. *Smart Materials and Structures, 28*, 12LT02.

31. Wei, C., & Jing, X. (2017). A comprehensive review on vibration energy harvesting: Modelling and realization. *Renewable Sustainable Energy Reviews, 74*, 1–18.

32. Yuan, T. C., Yang, J., & Chen, L. Q. (2018). Nonlinear dynamics of a circular piezoelectric plate for vibratory energy harvesting. *Communications in Nonlinear Science and Numerical Simulation, 59*, 651–656.

33. Zhang, L. B., Abdelkefi, A., Dai, H. L., et al. (2017). Design and experimental analysis of broadband energy harvesting from vortex-induced vibrations. *Journal of Sound and Vibration, 408*, 210–219.

34. Zhao, L. C., Zou, H. X., Yan, G., et al. (2018). Arbitrary-directional broadband vibration energy harvesting using magnetically coupled flex tensional transducers. *Smart Materials and Structures, 27*, 095010.

35. Zhou, S., & Wang, J. (2018). Dual serial vortex-induced energy harvesting system for enhanced energy harvesting. *AIP Advances, 8*, 075221.

36. Zhou, S. X., Cao, J. Y., Inman, D. J., et al. (2014). Broadband tristable energy harvester: Modeling and experiment verification. *Applied Energy, 133*, 33–39.

37. Zhou, S. X., & Zuo, L. (2018). Nonlinear dynamic analysis of asymmetric tristable energy harvesters for enhanced energy harvesting. *Communications in Nonlinear Science and Numerical Simulation, 61*, 271–284.

38. Zhou, Z., Qin, W., Zhu, P., et al. (2018). Scavenging wind energy by a Y-shaped bi-stable energy harvester with curved wings. *Energy, 153*, 400–412.

39. Zou, H. X., Zhao, L. C., Gao, Q. H., et al. (2019). Mechanical modulations for enhancing energy harvesting: Principles, methods and applications. *Applied Energy, 255*, 113871.

Xiangdong Ding is currently a Master student in College of Mechanical Engineering, Beijing University of Technology, China. His research interests is energy harvesting from flow-induced vibration.

Xiangying Guo received her PhD degree in the College of Mechanical Engineering, Beijing University of Technology, China, in 2011. She is currently an Associate Professor in the College of Mechanical Engineering. Her research interests are in nonlinear dynamics, composite structures and mechanical vibration.

Dongxing Cao received his PhD degree in the College of Mechanical Engineering, Beijing University of Technology, China, in 2007. He is currently a Professor in the College of Mechanical Engineering. His research interests are in nonlinear dynamics, vibration energy harvesting and vibration control.

Minghui Yao received her PhD degree in the College of Mechanical Engineering, Beijing University of Technology, China, in 2006. She is currently a Professor in the School of Artificial Intelligence, Tianjin Polytechnic University, Tianjin. Her research interests are in nonlinear dynamics, vibration energy harvesting and structure dynamics.